Leo Chen huei (Orcid ID: 0000-0003-1424-9694)
Ng Hooi Hooi (Orcid ID: 0000-0002-2370-0849)
Qin Cheng Xue (Orcid ID: 0000-0003-2169-2686)

ANNEXIN-A1 DEFICIENCY EXACERBATES PATHOLOGICAL REMODELLING OF THE MESENTERIC VASCULATURE IN INSULIN-RESISTANCE BUT NOT INSULIN-DEFICIENCY

Maria Jelinic[1,2*], Nicola Kahlberg[1*], Chen Huei Leo[1,3], Hooi Hooi Ng[1,3,5], Sarah Rosli[4], Minh Deo[4], Mandy Li[4], Siobhan Finlayson[4], Jesse Walsh[4], Laura J Parry[1], Rebecca H Ritchie[4,6,7#], and Cheng Xue Qin[4,6, 7#]

Running Title: Annexin-A1 Attenuates Vascular Remodelling

*Joint first authors

[#]Joint senior and corresponding authors

[1]School of BioSciences, University of Melbourne, Parkville, VIC 3010, Australia

[2]Department of Physiology, Anatomy and Microbiology, La Trobe University, Bundoora, VIC 3086, Australia

[3]Science, Maths & Technology, Singapore University of Technology & Design, Singapore 487372

[4]Baker Heart & Diabetes Institute, Melbourne, VIC 3004, Australia

[5]Department of Human and Molecular Genetics, Herbert Wertheim College of Medicine, Florida International University, Miami, FL 33199, United States.

[6]Department of Diabetes, Monash University, Clayton, VIC 3168, Australia

This is the author manuscript accepted for publication and has undergone full peer review but has not been through the copyediting, typesetting, pagination and proofreading process, which may lead to differences between this version and the Version of Record. Please cite this article as doi: 10.1111/bph.14927

This article is protected by copyright. All rights reserved.

Author Manuscript

[7]Department of Pharmacology and Therapeutics, University of Melbourne, Parkville, VIC 3010, Australia

Author Manuscript

This article is protected by copyright. All rights reserved.

Author Manuscript

CORRESPONDENCE:

Dr Cheng Xue Qin, PhD, Heart Failure Pharmacology, Baker Heart & Diabetes Institute, 75 Commercial Rd, Melbourne 3004 Australia. Adjunct Research Fellow (University of Melbourne). Phone+613-8532-1374; Fax+613-8532-1100; Email chengxuehelena.qin@baker.edu.au

Prof Rebecca Ritchie, PhD, FCSANZ, FAHA; NHMRC Senior Research Fellow, Head Heart Failure Pharmacology, Baker Heart & Diabetes Institute, 75 Commercial Rd, Melbourne 3004 Australia. Adjunct Professor (Monash University). Phone+613-8532-1392; Fax+613-8532-1100; Email rebecca.ritchie@baker.edu.au

This article is protected by copyright. All rights reserved.

Author Manuscript

Abstract

Background and purpose:

Arterial stiffness, a hallmark of diabetes, increases the risk of cardiovascular complications. Potential mechanisms that promote arterial stiffness in diabetes include oxidative stress, glycation and inflammation. The anti-inflammatory protein annexin-A1 (AnxA1) has cardioprotective properties, particularly in the context of ischaemia. However, the role of endogenous AnxA1 in the vasculature in both normal physiology and pathophysiology remains largely unknown. Hence, this study investigated the role of endogenous AnxA1 in diabetes-induced remodelling of mouse mesenteric vasculature.

Experimental approach:

Insulin-resistance was induced in male mice (*AnxA1*$^{+/+}$ and *AnxA1*$^{-/-}$) with the combination of streptozotocin (55mg/kg i.p. x 3 days) with high fat diet (42% energy from fat) or citrate vehicle with normal chow diet (20-weeks). Insulin-deficiency was induced in a separate cohort of mice using a higher total streptozocin dose (55mg/kg i.p. x 5 days) on chow diet (16-weeks). At study endpoint, mesenteric artery passive mechanics were assessed by pressure myography.

Key results:

Insulin-resistance induced significant outward remodelling, but had no impact on passive stiffness. Interestingly, vascular stiffness was significantly increased in *AnxA1*$^{-/-}$ mice when subjected to insulin-resistance. In contrast, insulin-deficiency induced outward remodelling and increased volume compliance in mesenteric arteries, regardless of genotype. In addition, the AnxA1/FPR axis is upregulated in both insulin-resistance and insulin-deficiency mice.

This article is protected by copyright. All rights reserved.

Conclusion and implications:

Our study provided the first evidence that endogenous AnxA1 may play an important vasoprotective role in the context of insulin-resistance. AnxA1-based therapies may be used to provide additional benefits over traditional anti-inflammatory strategies for reducing vascular injury in settings of diabetes.

Author Manuscript

This article is protected by copyright. All rights reserved.

Author Manuscript

Bullet point summary:

What is already known? The endogenous anti-inflammatory protein AnxA1 is cardioprotective against acute severe ischaemic insults.

What does the study address? The role of endogenous AnxA1 in diabetes-induced remodelling in mouse mesenteric vasculature.

Clinical significance: AnxA1-based strategies may represent a novel therapy to reduce vascular damage in diabetes, particularly those patients suffering from type 2 diabetes.

Keywords

Annexin-A1, diabetes, passive mechanical wall properties, outward remodelling, mesenteric artery.

Abbreviations

AnxA1	Annexin-A1 gene
AnxA1	Annexin-A1 protein
AUC	Area under curve
CSA	Cross-sectional area
HbA1c	Glycated haemoglobin
InsRes	Insulin-resistant
FPR	Formyl peptide receptor
STZ	Streptozotocin

This article is protected by copyright. All rights reserved.

T1D	Type 1 diabetes
T2D	Type 2 diabetes

Author Manuscript

This article is protected by copyright. All rights reserved.

Author Manuscript

INTRODUCTION

The passive mechanical wall properties of the vasculature play a vital role in assisting normal function of the cardiovascular system. When vessels stiffen, the ability of the vascular wall to recoil is reduced, increasing pulse pressure, which in turn damages the smaller peripheral vessels (Henry et al., 2003; Martinez-Lemus et al., 2009). Vascular stiffening is a hallmark of many cardiovascular diseases, where diabetes mellitus is a major risk factor (Henry, Kostense et al., 2003; Stehouwer et al., 2008; Zieman et al., 2005). In addition, vascular stiffness is a critical factor for the initial development of vascular complications in diabetes (Prenner et al., 2015; Wilkinson et al., 2001). Thus, developing novel strategies to target vascular stiffening offer significant therapeutic potential for the treatment of diabetic vascular complications.

There are three common types of diabetes – type 1, type 2 and gestational diabetes. The most common type of diabetes is Type 2 diabetes (T2D), often considered a lifestyle disease. It is commonly associated with a combination of factors including increased bodyweight, smoking, excessive alcohol intake and physical inactivity (Huynh et al., 2014; Zimmet et al., 2001). The sustained release of insulin from the pancreas in this context occurs in order to maintain homeostasis with elevated blood glucose concentrations, ultimately leading to insulin resistance (Zimmet, Alberti et al., 2001). In contrast, Type 1 diabetes (T1D) is an auto-immune disease characterised by the gradual destruction of pancreatic β-islet cells, resulting in insulin deficiency (Raskin et al., 2010; Zimmet, Alberti et al., 2001). The remodelling of the resistance vasculature (e.g. mesenteric arteries) in diabetes has been largely studied in rodent models of T1D. The general consensus from these studies is that diabetes induces outward hypertrophic remodelling in mesenteric arteries (Crijns et al., 1999;

This article is protected by copyright. All rights reserved.

Author Manuscript

Souza-Smith et al., 2011), largely attributed to increased oxidative stress and inflammatory response (Huynh, Bernardo et al., 2014; Zimmet, Alberti et al., 2001). We recently confirmed that streptozotocin (STZ)-induced T1D elicits outward hypertrophic remodelling and increased stiffness in rats with moderate (~20mM blood glucose) or severe hyperglycaemia (~30mM blood glucose) (Kahlberg et al., 2016). However, other reports suggest that diabetes increased circumferential stiffness only in the femoral artery, but not in mesenteric arteries (Wigg et al., 2004). In most studies, the impact of diabetes on vascular remodelling have focused in T1D models. Little is known regarding the impact of T2D on resistance vascular remodelling despite 90% of diabetic patients exhibiting T2D (Huynh, Bernardo et al., 2014; Zimmet, Alberti et al., 2001). Thus, further work is warranted to better understand the relative impact of insulin resistance versus insulin deficiency on vascular remodelling, particularly in resistance vessels.

Diabetes is a low-grade, chronic inflammatory disorder (Devaraj et al., 2010; Huynh, Bernardo et al., 2014). Circulating levels of inflammatory markers (such as C-reactive protein and pro-inflammatory cytokines) are increased in diabetic patients, as is monocyte adhesion to the endothelium (Hanley et al., 2004; Schalkwijk et al., 1999). Targeting this vascular inflammation, and the resolution of inflammatory pathways, may reduce adverse vascular remodelling in diabetes. Annexin-A1 (AnxA1) is a naturally occurring anti-inflammatory protein that belongs to the annexin superfamily (Perretti et al., 2009b; Qin et al., 2015). It is an important second messenger for glucocorticoids, and mediates many of their anti-inflammatory actions (Perretti et al., 2009a). Mice deficient in AnxA1 exhibit an exaggerated response to many inflammatory disorders, including pulmonary fibrosis (Damazo et al.,

This article is protected by copyright. All rights reserved.

Author Manuscript

2011), rheumatoid arthritis (Yang et al., 2004), stroke (Gavins et al., 2007), and endotoxemia (Damazo et al., 2005; Qin, Yang et al., 2015). This is consistent with our previous observations that exogenous AnxA1 preserves myocardial function in ischaemia-reperfusion injury *in vitro* (Qin et al., 2013; Ritchie et al., 2005; Ritchie et al., 2003).

AnxA1 is expressed in endothelial cells and vascular smooth muscle cells in the vasculature (Pan et al., 2016; Paravicini et al., 2009), where it exhibits anti-inflammatory properties (Pan, Kong et al., 2016). It has been demonstrated that the level of AnxA1 is elevated in individuals with type 1 diabetes, and deficiency in AnxA1 exhibits a more severe diabetic phenotype in the heart and kidney compare to diabetic wildtype mice (Purvis et al., 2018). In addition, the levels of AnxA1 is also elevated in patients with type 2 diabetes, and AnxA1 deficiency mice fed a high fat diet have more severe diabetic phenotype, including dyslipidaemia, insulin resistance (Purvis et al., 2019). However, the impact of AnxA1 deficiency on arterial wall stiffness has not been studied. The aim of the current study was to investigate the impact of AnxA1 deficiency on vascular remodelling and stiffness, in both insulin-resistant and insulin-deficient mice. We hypothesised that insulin resistance and deficiency exhibit differential adverse remodelling in the mesenteric vasculature, and that this is exacerbated in *AnxA1*$^{-/-}$ mice.

METHODS

Animals

This article is protected by copyright. All rights reserved.

Author Manuscript

All animal experiments complied with the National Health and Medical Research Council (NHMRC) of Australia code of practice for the care and use of animals for scientific purposes, ARRIVE guidelines and Directive 2010/63/EU of the European Parliament in the protection of animal used for scientific purpose. Animal care and experimental protocols were approved by the Alfred Medical Research and Educational Precinct (AMREP) Animal Ethics Committee (E/1535/2013/B). Male *AnxA1*$^{+/+}$ wildtype and *AnxA1*$^{-/-}$ mice (on a C57BL/6 background; Hannon et al., 2003) were bred and housed in individually ventilated cages (maximum 6 non-diabetic or 4 diabetic mice per cage) at the AMREP Animal Centre and maintained under a 12h light/dark cycle, with food and water provided *ad libitum* for study in two distinct models of diabetes, insulin deficiency and insulin resistance. Regular welfare-related assessments were carried out throughout the study. Specifically, mice were monitored daily. Animals identified as unwell were placed on an Animal Care form and any pain or ailments were treated accordingly. Animals that responded to treatment and fully recovered were allowed to continue in the study. Animals not responding at all to treatment or showing signs of ongoing deterioration within 24h, were removed from the remainder of the study and humanely euthanised.

Insulin resistance was induced in 6-weeks-old male *AnxA1*$^{-/-}$ and *AnxA1*$^{+/+}$ mice. Animals were randomly assigned to receive three consecutive daily *i.p*. injections of STZ (55mg/kg body weight, in 0.1M citrate vehicle, pH 4.5; Sigma-Aldrich, St Louis, MO, USA) with concomitant high fat diet (HFD, High fat diet SF04-001, 42% energy intake from lipids, Specialty Feeds, WA). The corresponding sham animals received three consecutive daily *i.p*. injections of citrate vehicle with concomitant chow diet. Blood glucose levels and body

This article is protected by copyright. All rights reserved.

Author Manuscript

weight were monitored every 2 weeks for a period of 20 weeks. Mice allocated to low-dose STZ/HFD that exhibited blood glucose levels of 12-20mM were considered to be insulin-resistant, whereas mice that were fed a normal diet and given citrate vehicle injections were considered as non-diabetic sham controls, and presented with blood glucose levels <12mM. Blood glucose and body weight were monitored fortnightly using a handheld glucometer (ACCU-CHEK Advantage, Roche, Basel, Switzerland) until endpoint (20 weeks of insulin resistance or sham). Glucose tolerance testing was conducted in 5-hour fasted mice *in vivo* one week prior to cull. After a baseline glucose reading, 25% glucose solution (Baxter, Viaflex®, *i.p.*) was injected as a single bolus at the beginning of each *i.p*. glucose tolerance experiment, after which blood glucose measurements were obtained via tail vein bleeds. Blood glucose was measured at baseline (0 minutes), 15, 30, 45, 60, 90 and 120 minutes after injection of glucose.

Insulin-deficient T1D was induced in a separate cohort of mice, using a higher total STZ dose, as previously described (Ng et al., 2017; Ritchie et al., 2012). Briefly, 6-week-old male *AnxA1*$^{-/-}$ and *AnxA1*$^{+/+}$ mice were randomly assigned to receive 5 consecutive daily *i.p.* injections of STZ, to induce insulin deficiency (55mg/kg body weight per day, in 0.1M citrate vehicle, pH 4.5; Sigma-Aldrich, St Louis, MO, USA) or 5 consecutive daily *i.p*. injections of citrate vehicle of equivalent volume (sham group), following an overnight fast. Both T1D and sham mice received chow diet. Insulin deficiency was confirmed in mice if blood glucose were >25mM at study endpoint. Blood glucose and body weight were monitored fortnightly using a handheld glucometer until endpoint (16 weeks of insulin-deficiency or sham).

This article is protected by copyright. All rights reserved.

Author Manuscript

In vivo analyses at study endpoint

Arterial blood pressures and heart rate were examined at experimental endpoint (16 and 20 weeks in the insulin-resistant and insulin-deficient studies, respectively). This was determined via catheterisation in anaesthetised mice (ketamine/xylazine/atropine: 100/10/1.2mg/kg i.p.) using a 1.4 Fr Millar MICRO-TIP pressure catheter and a Powerlab System (AD Instruments, Bella Vista, NSW, Australia) as described previously (Ritchie, Love et al., 2012). A Cobas HbA1c analyser (Roche, Sydney, NSW, Australia) was used to determine HbA1c levels. Plasma insulin levels were determined using a mouse insulin ELISA (cat# 80-INSMSU-E01) (ALPCO, Boston, US), according to the manufacturer's instructions. Multiple ELISA plates were required to assess all the plasma samples in the study. To limited plate-to-plate variation, data were expressed as mean fold change relative to the within-plate control group (*AnxA1*$^{+/+}$ sham).

Passive mechanical wall properties ex vivo

Following catheterisation, a section of the mesenteric arcade was immediately placed in an ice-cold Krebs' bicarbonate solution (mM: NaCl 120, KCl 5, $MgSO_4$ 1.2, KH_2PO_4 1.2, $NaHCO_3$ 25, D-glucose 11.1, $CaCl_2$ 2.5). First order mesenteric arteries were cleared of fat and connective tissue and leak-free segments were mounted on the cannula of a pressure myograph (Living Systems Instrumentation, Burlington, VT, USA), and placed in a Ca^{2+}-free physiological saline solution (PSS, mM: NaCl 14.9, KCl 4.7, $NaHCO_3$ 4.7, KH_2PO_4 1.2, $MgSO_4$ 1.7, glucose 5, HEPES 10 and EGTA 2). The lumen was gently flushed with PSS to remove any remaining blood, and the distal end of the artery was occluded and left free to allow it to lengthen passively with pressure.

This article is protected by copyright. All rights reserved.

Author Manuscript

Arteries were incubated at 37°C for 20 minutes prior to determination of vessel wall parameters. These included vessel length, outer diameter (OD) and wall thickness, in 10mmHg increments from 5mmHg to 120mmHg. Parameters were obtained using a Nikon Eclipse TS100 inverted microscope with a Hitachi KP-M3AN CCD camera attached. This was projected onto a monitor, and parameters were measured manually using a ruler, and then converted into microns using a conversion factor (calculated from measurements made using a graticule) measured on a screen. Inner diameter (ID), wall stress and wall strain were calculated as described previously (Jelinic et al., 2014). Wall cross-sectional area (CSA) was calculated as $((\pi \times OD^2)/4) - ((\pi \times ID^2)/4)$. Volume distensibility was calculated as Δ volume/([Δ cross-sectional area × length]× Δ Pressure), where cross-sectional area was calculated as $(\pi \times ID^2)/4$) (Leo et al., 2014). Volume compliance was calculated for each pressure increment using the following calculation: volume compliance = (Δ volume)/(Δ pressure), where Δ volume = (Δ CSA) × (Δ length), and cross sectional area = $(\pi \times ID^2)/4$ (Jelinic et al., 2015). The % change in length with pressure was calculated using the following equation: % length = [(value at pressure)/(value at baseline)] × 100 (Jelinic, Conrad et al., 2015).

Quantitative PCR

To further study the effects of AnxA1 on endothelium-dependent vasodilation and smooth muscle constriction, the expression of genes of interest [e.g *mouse formyl peptide receptor* 1(*mFpr1), mFpr2, mAnxA1, mMcp-1*), was analyzed. Frozen blood vessels (each n number

This article is protected by copyright. All rights reserved.

consisted of 1st and 2nd order mesenteric arteries from 1 – 2 mice) were placed in pre-chilled Wig-L-Bug® capsules with a silver ball bearing and pulverized in a Digital Wig-L-Bug® amalgamator (Dentsply-Rinn, Elgin, IL, USA). Pulverized tissues were resuspended in 1 ml TriReagent (Ambion Inc., Scoresbury, VIC, Australia) and total RNA was then extracted as described previously (Jelinic et al., 2017). RNA pellets were resuspended in 12 µl RNA Secure™ (Ambion). Quality and quantity of RNA was analyzed using the NanoDrop ND1000 Spectrophotometer (Thermo Fischer Scientific Australia Pty Ltd, Scoresby, VIC, Australia) with A_{260}:A_{280} ratios > 1.8 indicating sufficient quality for quantitative real-time polymerase chain reaction (qPCR) analysis. First strand cDNA synthesis was performed using the RT^2 First Strand Kit (QIAGEN, Maryland, USA) as per instructions using 0.5 µg of total RNA per reaction. The qPCR analysis of genes of interest was performed using RT^2 Profiler™ Custom PCR Array for Mouse (QIAGEN) as per kit instructions for the AB Applied Biosystems Biosystems 7500 Real-Time PCR System (Life Technologies, Mulgrave, VIC, Australia) in 20 µl volume reactions. β-actin (*Actb2*), β-2 microglobulin (*B2m*), and glyceraldehyde 3-phosphate dehydrogenase (*Gapdh*) were the reference genes, however, there were significant differences between groups for all of these genes and thus, for each diabetic setting, the control group (*AnxA1*$^{+/+}$ sham) was used as the internal calibrator and this was subtracted from the mean gene of interest triplicate CT value (Ratio(test/calibrator) = $2\Delta CT$, where $\Delta CT = CT(calibrator) - CT(test)$) as has been described previously (Marshall et al., 2016). These "normalised" data (ΔCT) were presented as fold induction relative to the control group (*AnxA1*$^{+/+}$ sham).

Immunohistochemistry

This article is protected by copyright. All rights reserved.

Author Manuscript

Author Manuscript

Immunohistochemistry has been conducted, the experimental detail are provided, these conform with BJP Guidelines (Alexander et al., 2018). Mouse mesenteric arteries (*AnxA1*$^{+/+}$ mice), were fixed in neutral-buffered formalin, embedded in paraffin (Alfred Pathology Service, Melbourne, VIC, Australia) and then sectioned at 4 µm. Sections were deparaffinised, rinsed and antigen retrieval was performed by incubating the slides for 20 min at 95 ºC in 0.01% citrate buffer. Sections were blocked in 5% NGS in 0.01% PBS/Tween 20 for 1h. To detect the expression of FPR1 and FPR2 in the vessel, sections were then incubated overnight at 4ºC with either FPR1 (1:100 in 5% NGS and 0.01% PBS-T, Biorbyt Cat# orb13410, RRID:AB_10752393, Cambridge, UK) or FPR2 primary antibody (1:100 in 5% NGS and 0.01% PBS-T, sc-66901, Bioss Cat# bs-3654R, RRID:AB_10858084, Texas, USA). Representative images were photographed as described previously (Qin et al., 2019). Positive FPR1 or FPR2 stained brown and was graded by a blinded observer as follows: score 0, negative stain; score 1, very weak; score 2, weak; score 3, moderate; score 4, intense; score 5, very intense. Three to five sections were assessed per mouse, and five to seven mice were analysed per group.

Data and analysis

The manuscript complies with BJP's recommendation and requirements on experimental design and analysis (Curtis et al., 2018). All data are expressed as mean ± SEM. All figure formatting and statistical analyses were undertaken using Prism version 5.0 (GraphPad Software, San Diego, CA, USA). Certain experiments were undertaken in duplicate (ELISA) to ensure the reliability of single values. Data analysis and data presentation from these experiments used the single values obtained from the mean of the technical replicates used.

This article is protected by copyright. All rights reserved.

Author Manuscript

'n' refers to number of animals (independent values), not replicates or independent experiments. For all experimental protocols, sample sizes were based on the number required to provide >80% power to detect an effect size of 20% at P<0.05. All analyses were performed blinded whereby animal ID was known by the investigator but the experimental group of the animal was not revealed until after analyses were performed. Body weight, blood glucose levels, stress-strain and wall parameters (inner and outer diameter, wall thickness and arterial lengthening) were analysed using repeated-measures two-way ANOVA with Bonferroni *post hoc* analysis. *Post-hoc* analysis was only performed when the F value was greater than F critical value, indicating that there was no variance in homogeneity. HbA1c levels, plasma insulin, area-under-curve (AUC), and gene expression were analysed using a two-way ANOVA, with Fisher's LSD *post-hoc* analysis. Student's t-test was used for *AnxA1* gene expression, and a Mann-Whitney test to quantify FPR1 and FPR2 protein immunostaining. $P<0.05$ was considered statistically significant. All groups analysed in this study have $n\geq5$. On occasion outliers were excluded in data analysis and presentation, where indicated on the Figure Legend. Outlier is predefined when an individual data point is 2 standard deviations away from the mean.

Nomenclature of Targets and Ligands

Key protein targets and ligands in this article are hyperlinked to corresponding entries in http://www.guidetopharmacology.org, the common portal for data from the IUPHAR/BPS Guide to PHARMACOLOG (Harding et al., 2018), and are permanently archived in the Concise Guide to PHARMACOLOGY 2017/18 (Alexander et al., 2017).

This article is protected by copyright. All rights reserved.

Author Manuscript

RESULTS

Insulin resistance mouse model

Systemic characteristics in vivo

The insulin resistance model was established using a combination of low dose STZ and HFD. This combination regimen did not reduce plasma insulin levels but resulted in a gradual rise in blood glucose levels, similar to that observed in insulin-resistant humans (Huynh, Bernardo et al., 2014; Mukherjee et al., 2013). There were no differences in body weight between any of the experimental groups in the insulin resistance study, whether sham or insulin-resistant mice (20 weeks of high fat diet superimposed with low-dose STZ, Fig 1A). Blood glucose levels were significantly elevated in both *AnxA1*$^{+/+}$ and *AnxA1*$^{-/-}$ insulin-resistant mice (Fig 1B). Notably, this level of hyperglycaemia was to a lesser extent than observed in insulin-deficient mice. Similarly, both *AnxA1*$^{+/+}$ and *AnxA1*$^{-/-}$ insulin-resistant mice exhibited significantly increased blood glucose levels during glucose tolerance tests, compared with shams (Fig 1E & 1F). Interestingly, HbA1c levels were increased significantly in *AnxA1*$^{+/+}$ insulin-resistant mice, but not in their corresponding *AnxA1*$^{-/-}$ counterparts. *Post hoc* analyses revealed that InsRes *AnxA1*$^{+/+}$ mice exhibited significantly increased blood glucose levels from 8 weeks after the induction of diabetes, whereas InsRes *AnxA1*$^{-/-}$ mice only exhibited increased plasma blood glucose levels from 16 weeks after the induction of diabetes. This could explain why the HbA1c levels were not significantly elevated in the *AnxA1*$^{-/-}$ group, because fasting blood glucose levels were only raised in the final 4 weeks [much less than the lifespan of a red blood cell (3 months)].

This article is protected by copyright. All rights reserved.

Author Manuscript

This suggests that the impairment in glycaemic control was less severe in *AnxA1*$^{-/-}$ mice subjected to insulin resistance (Fig 1C). In addition, plasma insulin levels only tended to be increased in *AnxA1*$^{-/-}$ insulin-resistant mice (Fig 1D). Collectively, these data confirm that the combination of low-dose STZ and HFD combination induced insulin resistance (elevated blood glucose levels, without impact on circulating insulin levels). Blood pressure and heart rate were measured in anaesthetised mice *in vivo* at study endpoint. Neither insulin resistance nor *AnxA1* deficiency significantly influenced systolic or diastolic blood pressure (Table 1). However, heart rate was significantly increased in *AnxA1*$^{-/-}$ insulin-resistant mice compared with *AnxA1*$^{-/-}$ shams (Table 1).

Passive mechanical wall properties of mesenteric vasculature ex vivo

Mesenteric artery passive inner diameter, outer diameter and wall cross-sectional area were significantly increased (with pressurisation) in *AnxA1*$^{+/+}$ insulin-resistant mice compared with all three other experimental groups (Fig 2A, 2B & 2D). No differences in wall thickness were observed between groups in the insulin resistance study (Fig 2C). These findings are indicative of hypertrophic outward remodelling (increased inner diameter and wall cross-sectional area) in *AnxA1*$^{+/+}$insulin-deficient mice, but *AnxA1* deficiency appears to impede this remodelling. Analysis of the stress-strain relationship indicated that there was no impact of either insulin resistance or *AnxA1* deficiency on mesenteric artery circumferential stiffness (Fig 3A). Passive volume compliance was also not affected by insulin resistance in either *AnxA1*$^{+/+}$ or *AnxA1*$^{-/-}$ mice. However, *AnxA1*$^{-/-}$ mice exhibited significantly reduced volume compliance compared with *AnxA1*$^{+/+}$ mice. *Post-hoc* analyses revealed this was only significant at 40mmHg in sham animals, and in mid-range pressures (40-60mmHg) in

This article is protected by copyright. All rights reserved.

Author Manuscript

insulin-resistant mice (Fig 3B & 3C). Hence, our data suggest that *AnxA1* deficiency alone reduced volume compliance in mesenteric artery, and that this is further exacerbated in mesenteric arteries from insulin-resistant mice. Mesenteric arteries from non-diabetic *AnxA1*$^{+/+}$ mice exhibited a significantly greater capacity to lengthen with pressurisation compared with all three other experimental groups studied (Fig 3D). This indicates that insulin resistance and *AnxA1* deficiency impedes on the ability of the mesenteric artery to lengthen with pressurisation.

Insulin-deficient mouse model

Systemic characteristics in vivo

In contrast to the above context of insulin resistance, high-dose STZ-induced insulin deficiency significantly impeded body weight gain, in both *AnxA1*$^{+/+}$ and *AnxA1*$^{-/-}$ mice (Fig 4A). Furthermore, this trend for retarded body weight gain was more apparent in *AnxA1*$^{-/-}$ insulin-deficient mice compared with *AnxA1*$^{+/+}$ insulin-deficient mice ~~($P<0.001$)~~. As expected, insulin deficiency significantly increased blood glucose and glycated haemoglobin (HbA1c) levels, in both *AnxA1*$^{+/+}$ and *AnxA1*$^{-/-}$ mice (Fig 4B & 4C). Plasma insulin levels were significantly decreased in *AnxA1*$^{+/+}$ insulin-deficient mice (Fig 4D), when compared to sham, confirming insulin deficiency. AnxA1 deficiency had no effect on blood glucose levels in non-diabetic sham mice, however plasma insulin levels were significantly reduced in *AnxA1*$^{-/-}$ sham mice, comparable to that of *AnxA1*$^{-/-}$ insulin-deficient mice (Fig 4D). Blood pressure and heart rate were measured in anaesthetised mice *in vivo* at study endpoint. Systolic blood pressure was significantly lower in insulin-deficient mice compared to sham mice, regardless of genotype (Table 1). Diastolic blood pressure and heart rate were not

This article is protected by copyright. All rights reserved.

Author Manuscript

significantly different across all four experimental groups in the insulin deficiency study (Table 1).

Passive mechanical wall properties of mesenteric vasculature ex vivo

Mesenteric artery passive inner and outer diameters were significantly increased (with pressurisation) in both *AnxA1*$^{+/+}$ and *AnxA1*$^{-/-}$ insulin-deficient mice throughout the whole pressurization range (Fig 5A & 5B). Conversely, there were no differences in wall thickness between all experimental groups in the insulin deficiency study (Fig 5C). Although vessel wall cross-sectional area was increased (with pressurisation) in insulin-deficient mice, this was only significant in *AnxA1*$^{+/+}$ mice (Fig 5D). Together, these findings suggest hypertrophic outward remodelling in *AnxA1*$^{+/+}$, and eutrophic remodelling (increased inner diameter but no change in cross-sectional area) in *AnxA1*$^{-/-}$ mice, in the context of insulin deficiency. There were no significant differences in the stress-strain relationship of the mesenteric arteries between *AnxA1*$^{-/-}$ and *AnxA1*$^{+/+}$ sham mice, nor between sham and insulin-deficient *AnxA1*$^{+/+}$ mice. Conversely, the stress-strain curve was significantly shifted to the right in *AnxA1*$^{-/-}$ insulin-deficient mice (compared with all three other experimental groups), indicating reduced circumferential stiffness (Fig 6A). Surprisingly, insulin-deficiency significantly increased volume compliance in mesenteric arteries, independent of genotype (both *AnxA1*$^{+/+}$ and *AnxA1*$^{-/-}$ mice), indicating a possible compensatory reduction in longitudinal stiffness (Fig 6B & 6C). Although there was no effect of AnxA1 deficiency on volume compliance, there were differences between genotypes in arterial lengthening. Specifically, percentage change in length with pressurisation was significantly increased in *AnxA1*$^{+/+}$ insulin-deficient mice compared with *AnxA1*$^{+/+}$ shams. Conversely, no differences

This article is protected by copyright. All rights reserved.

in arterial lengthening were observed between sham and insulin-deficient *AnxA1*$^{-/-}$ mice (Fig 6D).

The role of the AnxA1 pathway in insulin resistance and insulin deficiency

To further investigate the vascular role of AnxA1 in the settings of insulin resistance and insulin deficiency, we measured *mAnxA1*, *mFpr1* and *mFpr2* gene expression. Interestingly, we found that *mAnxA1* expression is significantly upregulated in both insulin-resistant and insulin-deficient *AnxA1*$^{+/+}$ mice (Fig 7A). *mFpr1* expression is upregulated in both insulin-deficient and insulin-resistant mice, whereas *mFpr2* is only significantly increased in insulin-deficient mice, regardless of genotype (Fig 7B, C), as revealed by two-way ANOVA. *Post-hoc* analysis revealed >5-fold upregulation of mFpr1 in *AnxA1*$^{-/-}$ mice compared to their wildtype counterparts (P<0.05, Fisher's LSD *post-hoc* analysis). We also measured a key pro-inflammatory cytokine *mMcp-1*. Consistent with the increased AnxA1/FPR axis, a significant upregulation of *mMCP-1* is observed in insulin-resistant and insulin-deficient mice. Interestingly, deficiency in *AnxA1* leads to increased *mFpr1*, *mMcp-1* in insulin-resistant mice. An outlier in insulin-deficient *AnxA1*$^{-/-}$ mice was identified and thus excluded for further analysis. We performed immunohistochemistry to localise FPR1 and FPR2 in the mesenteric artery. Both FPR1 and FPR2 were present in the vascular smooth muscle cells, and limited in endothelial cells, in the representative images obtained in the sham wild type mice. FPR2 staining was stronger than FPR1 (P<0.05, Mann-Whitney test), suggesting that there may be more prominent role for FPR2 in the mesenteric artery than FPR1 (Fig 7D). Control serum revealed no staining.

This article is protected by copyright. All rights reserved.

Author Manuscript

Author Manuscript

DISCUSSION AND CONCLUSIONS

The main finding of this study is the contribution of endogenous AnxA1 on mesenteric artery structure, with the extent of the impact being dependent on the phenotype of diabetes. Our study is the first to localise receptors for AnxA1 (FPR1 and FPR2) in the vascular smooth muscle of mesenteric arteries. Intriguingly, our findings suggest that deficiency of *AnxA1* exacerbated the development of key characteristics of vascular stiffness (reduced artery compliance) only in the setting of insulin resistance, but not insulin deficiency. Thus, our study demonstrates for the first time that *AnxA1* deficiency is detrimental to the vasculature in the setting of insulin resistance.

The insulin-resistant and insulin-deficient animal models of diabetes used in this study resulted in distinct differences between vascular phenotypes (as summarised in Fig 8 and Table 2). Specifically, insulin-deficient mice exhibited hyperglycaemia throughout the whole treatment period, with retarded body weight gain and reduced circulating insulin levels by study endpoint. Conversely, insulin-resistant mice exhibited a delayed, and much milder level of, hyperglycaemia, which was even milder in the *AnxA1*$^{-/-}$ mice. This is surprising considering that *AnxA1* deficiency exacerbated pathological remodelling in the context of insulin resistance, despite this delayed, milder hyperglycaemia. Despite a concomitant impairment in glucose tolerance, there were no differences in body weight or plasma insulin levels in insulin-resistant mice. Thus, our study represents two distinct disease settings, severe hyperglycaemia with insulin deficiency in both *AnxA1*$^{+/+}$ and *AnxA1*$^{-/-}$ mice (analogous

This article is protected by copyright. All rights reserved.

to T1D), and mild hyperglycaemia with insulin resistance in both genotypes. These differences may contribute to the differential vascular phenotypes observed in the two scenarios.

Previous report demonstrated that FPR2 mRNA is detectable in endothelial cells (HUVECs) and sections of lung tissue (Koczulla et al., 2003). We have however now provided immunostaining data to show the FPRs are present in the mesenteric artery in *AnxA1*$^{+/+}$ mice. Importantly, this is the first report to localise AnxA1 receptors (FPR1 and FPR2) to the mesenteric vasculature. Our data suggest that FPR2 is more prominent than FPR1 in this vascular bed and provides some of the first evidence that AnxA1 could be acting directly on the vascular smooth muscle cells to elicit vasoprotective effects in the mesenteric artery. Our study is also the first to show that *AnxA1* deficiency may exacerbate vascular remodelling specifically in the context of diabetes, an effect that is dependent on the nature of the diabetic phenotype; insulin deficiency versus insulin resistance. Despite the differences observed between the two models of diabetes, gene expression of *AnxA1*, its receptors *Fprs* and the key inflammatory cytokine *Mcp-1* were upregulated in the mesenteric vasculature in both insulin deficiency and insulin resistance. Interestingly, deficiency of *AnxA1* is sufficient to create a pro-inflammatory environment in the microvasculature. However, given the limited availability of remaining tissue, we are unable to provide further information at the protein level. Further studies are warranted to interrogate detailed mechanism that contributes to vascular remodelling in diabetic mice deficient in *AnxA1*.

This article is protected by copyright. All rights reserved.

Author Manuscript

Author Manuscript

The impact of AnxA1 on vascular remodelling has been studied in other cardiovascular pathologies (e.g. atherosclerosis), but not in the specific context of diabetes. Previous reports demonstrated that the response of *ApoE*$^{-/-}$ mice fed a high-cholesterol diet subjected to wire injury, particularly at the level of neointima thickness, is aggravated by the absence of endogenous AnxA1 (de Jong et al., 2017). Exogenous AnxA1 administration attenuates progression of established atherosclerotic plaques in mice fed a western type diet superimposed on low-density lipoprotein receptor deficiency (LDLR$^{-/-}$) (Kusters et al., 2015), but the impact of AnxA1 on vascular remodelling (away from regions of plaque) was not determined. Neither of these previous studies examined the impact of AnxA1 (endogenous or exogenous) on arterial passive mechanics, volume compliance or arterial stiffness, nor was the impact on resistance (as opposed to conduit) arteries examined.

In the mesenteric arteries of *AnxA1*$^{+/+}$ mice, insulin-deficient mice were associated with reduced axial stiffness, whereas insulin resistance had no effect on stiffness or compliance. These observations are consistent with our recent study in STZ-induced T1D rats, in which both moderate (20mM blood glucose) and severe hyperglycaemia (30mM blood glucose) increased axial, but not circumferential, stiffness in mesenteric arteries (Kahlberg, Qin et al., 2016). However, the impact of T1D on vascular stiffness remains controversial, as arterial stiffness was observed in rat cremaster arterioles (Hill et al., 1994), and femoral artery, but had no effect in mesenteric arteries (Wigg, Tare et al., 2004). Different phenotypes of diabetes exhibit varying effects in different vascular beds; discrepancies in the literature may also reflect the use of different animal strains (Wistar versus Sprague Dawley) or species (rats versus mice). Our study is consistent with published studies in that body weight gain was

This article is protected by copyright. All rights reserved.

Author Manuscript

retarded in insulin-deficient rats (Kahlberg, Qin et al., 2016). Interestingly, the STZ/HFD-induced insulin-resistant mice did not exhibit retarded body weight gain. It is possible that the high-fat diet may compensate for potential retarded weight gain as a result of the administration of low dose of STZ. High dose of STZ administration has been associated with retarded weight gain (Kahlberg, Qin et al., 2016).

One possible explanation that accounts for the difference in vascular phenotype observed between the two mouse models is body weight, which is an important contributing factor to haemodynamic (and in turn net vascular remodelling and passive mechanics) (Doevendans et al., 1998). In the present investigation, diabetes was induced from six weeks of age, when mice were still in a growth phase, with retarded body weight gain in the insulin-deficient mice. Substantial (~20%) vascular development also occurs in the mesenteric vasculature during this growth phase (Unthank et al., 1987), both circumferentially and axially. Thus, the impact of this altered weight gain in the insulin-deficient mice during this growth phase may have contributed to vascular remodelling observed in these mice. InsDef mice exhibited retarded body weight gain, consistent with our previous report in this model (Ng, Leo et al., 2017). Interestingly, *AnxA1*$^{-/-}$ mice exhibited lower body weight at study commencement, compare to *AnxA1*$^{+/+}$ mice. We suggest the difference between the InsDef *AnxA1*$^{+/+}$ and *AnxA1*$^{-/-}$ mice is predominantly due to the lower starting bodyweight, rather than deficiency in insulin. Similarly, high fat diet-induced bodyweight gain also impacts vascular remodelling, by promoting vascular stiffness in the aorta and mesenteric arteries (Foote et al., 2016; Santana et al., 2014), further supporting the influence of bodyweight on vascular remodelling and passive mechanics in this study. Hence, the retarded body weight gain in

This article is protected by copyright. All rights reserved.

Author Manuscript

insulin-deficient mice may reflect an adaptive, compensatory mechanism rather than a pathological response. Given that the blood supply to the mesentery increases in diabetes (Hill et al., 1989), and that the insulin-deficient mice studied here exhibited lower blood pressure compare to control (at least under anaesthesia), this observation is consistent with reduced mesenteric artery axial stiffness in these mice. Despite increased mesenteric artery stiffness in insulin-resistant mice, deficiency in *AnxA1* did not impact blood pressure measurements (under anaesthesia). This could be due to compensatory effects on vascular function or haemodynamics, further studies are required to elucidate these mechanisms. The impact of AnxA1 deficiency on blood pressure in conscious animals remains to be investigated in future studies.

A number of previous studies have reported that mesenteric arteries from both insulin-deficient (Crijns, Wolffenbuttel et al., 1999; Kahlberg, Qin et al., 2016; Pourageaud et al., 1997) and insulin-resistant rodents (Souza-Smith, Katz et al., 2011) undergo hypertrophic outward remodelling. We also observed this phenomenon in *AnxA1*$^{+/+}$ mice from both insulin-resistant and insulin-deficient models of diabetes. In contrast, *AnxA1*$^{-/-}$ mice exhibited different types of vascular remodelling, dependent on the disease phenotype. Insulin deficiency induced eutrophic outward remodelling in *AnxA1*$^{-/-}$ mice, accompanied by reduced arterial stiffness, suggesting that AnxA1 deficiency may not be detrimental in the context of T1D. This suggests that there may be compensatory mechanisms in the vasculature of *AnxA1*$^{-/-}$ mice to enable them to better adapt to the challenge of insulin deficiency. Insulin resistance had no impact on artery wall parameters in *AnxA1*$^{-/-}$ mice, but was associated with a reduction in volume compliance. This indicates that in the absence of AnxA1, volume compliance is

This article is protected by copyright. All rights reserved.

Author Manuscript

compromised in the setting of insulin resistance. Furthermore, *AnxA1*$^{-/-}$ InsRes mice and *AnxA1*$^{+/+}$ sham mice are significantly different at low intraluminal pressure (40mmHg), suggesting that AnxA1 might play an important physiological role in regulating mesenteric arterial stiffness. It has been suggested that reduction in arterial compliance may precede (and exacerbate) the onset of diseases such as hypertension and atherosclerosis, and may help to identify individuals at risk before the onset of symptom (Glasser et al., 1997). Another potential explanation for why *AnxA1* deficiency exerted different effects in the two different models of diabetes is that AnxA1 is endogenously expressed in the islets of the pancreas, where it co-localises with insulin secretory granules, and has been suggested to influence glucose-stimulated insulin secretion in an autocrine or paracrine manner (Ohnishi et al., 1995). In addition, AnxA1 is known modulate islet function to enhance glucose-stimulated insulin secretion (Rackham et al., 2016). In InsDef mice, secretion is reduced, whereas in the InsRes mice, secretion is maintained (and likely eventually increases). It is thus possible that Anx-A1 deficiency leads to dysregulation of insulin secretion, resulting in elevated insulin plasma level in insulin-resistant mice. This may explain why *AnxA1* deficiency exerts differential effects in the two different models of diabetes.

Importantly, *AnxA1*$^{-/-}$ insulin-resistant mice also exhibited increased heart rate, which could potentially reflect increased activation of the sympathetic nervous system (as occurs in the human setting of diabetes), which may also contribute to the observed reduction in volume compliance (Bellien et al., 2010; Sasson et al., 2012). Although such a possibility was beyond the scope of the present study, previous reports in T2D mice demonstrate that haemodynamic changes precede mesenteric artery remodelling (Raskin & Mohan, 2010). Nevertheless, our

This article is protected by copyright. All rights reserved.

Author Manuscript

study suggests that *AnxA1* deficiency is detrimental to the mesenteric vasculature in insulin resistance. Thus, endogenous AnxA1 may play a protective role in the settings of insulin resistance, supporting the potential use of AnxA1 pharmacotherapy to alleviate microvascular complications in type 2 diabetes.

The results presented here indicate that insulin deficiency induces outward remodelling and reduced axial stiffness, in both $AnxA1^{+/+}$ and $AnxA1^{-/-}$ mice. In contrast, insulin resistance has differential effects depending on the genotype. $AnxA1^{+/+}$ mice with insulin resistance exhibit outward remodelling but not vascular stiffness. Conversely, insulin-resistant $AnxA1^{-/-}$ mice exhibit stiffer mesenteric arteries, with no difference in wall parameters. Our study is the first to compare systemic resistance artery stiffness in models of insulin resistance and insulin deficiency. Furthermore, we demonstrated for the first time that endogenous AnxA1 exaggerates vascular stiffness specifically in insulin-resistant mice, consistent with the anti-inflammatory properties of AnxA1. Limited availability of mesenteric artery tissue however precludes whether this this increased vascular stiffness was associated with increased intima-media thickness or collagen deposition. Further studies are now warranted to identify the full impact of endogenous AnxA1 in the vasculature and the associated molecular mechanisms by which it acts, particularly in the context of insulin resistance. Whether the increased mesenteric vascular stiffness evident in $AnxA1^{-/-}$ insulin-resistant mice could be rescued by exogenous AnxA1 or its mimetic remains to be determined. AnxA1-based strategies may represent a novel therapy to reduce vascular damage in patients suffering diabetes.

This article is protected by copyright. All rights reserved.

Author Manuscript

In conclusion, our data reveals that endogenous AnxA1 has diabetes-specific effects on mesenteric artery passive mechanics (summarised in Fig 8). This observation is the first study to examine the contribution of endogenous AnxA1 to passive mechanic wall properties in the context of insulin resistance *in vivo*. Our data reveals compelling new insights for the development of AnxA1-based strategies for treating vascular stiffness in patients associated with insulin resistance.

ACKNOWLEDGEMENTS

The research was funded by the CASS foundation (CXQ), the National Health and Medical Research Council (RHR, ID1081770), the Jack Brockhoff Foundation and part of the Victorian Government of Australia's Operational Infrastructure Support Program. RHR is a NHMRC Senior Research Fellow (ID1059960) and MJ is a joint NHMRC and National Heart Foundation Early Career Research Fellow. NK received a Melbourne Research Scholarship, CHL received the JN Peter's Research Fellowship, HHN received a Melbourne International Research Scholarship and a Melbourne International Fee Remission Scholarship and CXQ received a Baker Fellowship. We also thank Dr Helen Kiriazis for performing catheterisation and Ms Kelly O'Sullivan for technical assistance in this study. No other persons have made substantial contributions to this manuscript.

This article is protected by copyright. All rights reserved.

Author Manuscript

AUTHOR CONTRIBUTIONS

MJ, NK, CHL, CXQ and RHR designed the research, MJ, NK, CHL, HHN, SR, MD, ML, SF and CXQ collected and analysed the data, MJ, CHL, HHN, LJP, CXQ and RHR interpreted the data. MJ, NK, JW, LJP, CXQ and RHR drafted the manuscript. All authors approved the final version of the manuscript.

CONFLICT OF INTEREST

The authors declare no conflicts of interest.

DECLARATION OF TRANSPARENCY AND SCIENTIFIC RIGOUR

This Declaration acknowledges that this paper adheres to the principles for transparent reporting and scientific rigour of preclinical research as stated in the BJP guidelines for Design & Analysis, Immunoblotting and Immunochemistry, and Animal Experimentation, and as recommended by funding agencies, publishers and other organisations engaged with supporting research.

This article is protected by copyright. All rights reserved.

Author Manuscript

References:

Alexander SP, Kelly E, Marrion NV, Peters JA, Faccenda E, Harding SD, *et al.* (2017). THE CONCISE GUIDE TO PHARMACOLOGY 2017/18: Overview. Br J Pharmacol 174 Suppl 1**:** S1-S16.

Alexander SPH, Roberts RE, Broughton BRS, Sobey CG, George CH, Stanford SC, *et al.* (2018). Goals and practicalities of immunoblotting and immunohistochemistry: A guide for submission to the British Journal of Pharmacology. Br J Pharmacol 175**:** 407-411.

Bellien J, Favre J, Iacob M, Gao J, Thuillez C, Richard V, *et al.* (2010). Arterial stiffness is regulated by nitric oxide and endothelium-derived hyperpolarizing factor during changes in blood flow in humans. Hypertension 55**:** 674-680.

Crijns FRL, Wolffenbuttel BHR, De Mey JGR, & Boudier H (1999). Mechanical properties of mesenteric arteries in diabetic rats: consequences of outward remodeling. Am J Physiol 276**:** H1672-H1677.

Curtis MJ, Alexander S, Cirino G, Docherty JR, George CH, Giembycz MA, *et al.* (2018). Experimental design and analysis and their reporting II: updated and simplified guidance for authors and peer reviewers. Br J Pharmacol 175**:** 987-993.

Damazo AS, Sampaio AL, Nakata CM, Flower RJ, Perretti M, & Oliani SM (2011). Endogenous annexin A1 counter-regulates bleomycin-induced lung fibrosis. BMC Immunol 12**:** 59-59.

Damazo AS, Yona S, D'Acquisto F, Flower RJ, Oliani SM, & Perretti M (2005). Critical protective role for annexin 1 gene expression in the endotoxemic murine microcirculation. Am J Pathol 166**:** 1607-1617.

de Jong RJ, Paulin N, Lemnitzer P, Viola JR, Winter C, Ferraro B, *et al.* (2017). Protective aptitude of Annexin A1 in arterial neointima formation in atherosclerosis-prone mice. Arterioscler Thromb Vasc Biol 37**:** 312-315.

Devaraj S, Dasu MR, & Jialal I (2010). Diabetes is a proinflammatory state: a translational perspective. Expert Rev Endocrinol Metab 5**:** 19-28.

Doevendans PA, Daemen MJ, de Muinck ED, & Smits JF (1998). Cardiovascular phenotyping in mice. Cardiovasc Res 39**:** 34-49.

Foote CA, Castorena-Gonzalez JA, Ramirez-Perez FI, Jia G, Hill MA, Reyes-Aldasoro CC, *et al.* (2016). Arterial Stiffening in Western Diet-Fed Mice Is Associated with Increased Vascular Elastin, Transforming Growth Factor-β, and Plasma Neuraminidase. Front Physiol 7**:** 285-285.

Gavins FNE, Dalli J, Flower RJ, Granger DN, & Perretti M (2007). Activation of the annexin 1 counter-regulatory circuit affords protection in the mouse brain microcirculation. FASEB J 21**:** 1751-1758.

This article is protected by copyright. All rights reserved.

Author Manuscript

Glasser SP, Arnett DK, McVeigh GE, Finkelstein SM, Bank AJ, Morgan DJ, *et al.* (1997). Vascular compliance and cardiovascular disease: a risk factor or a marker? Am J Hypertens 10**:** 1175-1189.

Hanley AJG, Festa A, D'Agostino RBJ, Wagenknecht LE, Savage PJ, Tracy RP, *et al.* (2004). Metabolic and inflammation variable clusters and prediction of type 2 diabetes: factor analysis using directly measured insulin sensitivity. Diabetes 53**:** 1773-1782.

Hannon R, Croxtall JD, Getting SJ, Roviezzo F, Yona S, Paul-Clark MJ, *et al.* (2003). Aberrant inflammation and resistance to glucocorticoids in annexin 1-/- mouse. FASEB J 17**:** 253-255.

Harding SD, Sharman JL, Faccenda E, Southan C, Pawson AJ, Ireland S, *et al.* (2018). The IUPHAR/BPS Guide to PHARMACOLOGY in 2018: updates and expansion to encompass the new guide to IMMUNOPHARMACOLOGY. Nucleic Acids Res 46**:** D1091-D1106.

Henry RMA, Kostense PJ, Spijkerman AMW, Dekker JM, Nijpels G, Heine RJ, *et al.* (2003). Arterial stiffness increases with deteriorating glucose tolerance status: the Hoorn Study. Circ 107**:** 2089-2095.

Hill MA, & Ege EA (1994). Active and passive mechanical properties of isolated arterioles from STZ-induced diabetic rats: effect of aminoguanidine treatment. Diabetes 43**:** 1450-1456.

Hill MA, & Larkins RG (1989). Alterations in distribution of cardiac output in experimental diabetes in rats. Am J Physiol 257**:** H571-H580.

Huynh K, Bernardo BC, McMullen JR, & Ritchie RH (2014). Diabetic cardiomyopathy: Mechanisms and new treatment strategies targeting antioxidant signaling pathways. Pharmacol Ther 142**:** 375-415.

Jelinic M, Conrad KP, Tare M, & Parry LJ (2015). Differential effects of relaxin deficiency on vascular aging in arteries of male mice. AGE 37**:** 9803.

Jelinic M, Leo CH, Marshall SA, Senadheera SN, Parry LJ, & Tare M (2017). Short-term (48 hours) intravenous serelaxin infusion has no effect on myogenic tone or vascular remodeling in rat mesenteric arteries. Microcirculation 24.

Jelinic M, Leo CH, Post Uiterweer ED, Sandow SL, Gooi JH, Wlodek ME, *et al.* (2014). Localization of relaxin receptors in arteries and veins, and region-specific increases in compliance and bradykinin-mediated relaxation after in vivo serelaxin treatment. FASEB J 28**:** 275-287.

Kahlberg N, Qin CX, Anthonisz J, Jap E, Ng HH, Jelinic M, *et al.* (2016). Adverse vascular remodelling is more sensitive than endothelial dysfunction to hyperglycaemia in diabetic rat mesenteric arteries. Pharmacol Res 111**:** 325-335.

Koczulla R, von Degenfeld G, Kupatt C, Krotz F, Zahler S, Gloe T, *et al.* (2003). An angiogenic role for the human peptide antibiotic LL-37/hCAP-18. J Clin Invest 111**:** 1665-1672.

Kusters DH, Chatrou ML, Willems BA, De Saint-Hubert M, Bauwens M, van der Vorst E, *et al.* (2015). Pharmacological treatment with Annexin A1 reduces atherosclerotic plaque burden in LDLR-/- mice on western type diet. PLoS One 10**:** e0130484.

This article is protected by copyright. All rights reserved.

Author Manuscript

Leo CH, Jelinic M, Gooi JH, Tare M, & Parry LJ (2014). A vasoactive role for endogenous relaxin in mesenteric arteries of male mice. PLoS ONE 9**:** 1-12.

Marshall SA, Ng L, Unemori EN, Girling JE, & Parry LJ (2016). Relaxin deficiency results in increased expression of angiogenesis- and remodelling-related genes in the uterus of early pregnant mice but does not affect endometrial angiogenesis prior to implantation. Reprod Biol Endocrinol 14**:** 11.

Martinez-Lemus LA, Hill MA, & Meininger GA (2009). The plastic nature of the vascular wall: a continuum of remodeling events contributing to control of arteriolar diameter and structure. Physiology 24**:** 45-57.

Mukherjee B, Hossain CM, Mondal L, Paul P, & Ghosh MK (2013). Obesity and Insulin Resistance: An Abridged Molecular Correlation. Lipid insights 6**:** 1-11.

Ng HH, Leo CH, Prakoso D, Qin C, Ritchie RH, & Parry LJ (2017). Serelaxin treatment reverses vascular dysfunction and left ventricular hypertrophy in a mouse model of Type 1 diabetes. Sci Rep 7**:** 39604.

Ohnishi M, Tokuda M, Masaki T, Fujimura T, Tai Y, Itano T, *et al.* (1995). Involvement of annexin-I in glucose-induced insulin secretion in rat pancreatic islets. Endocrinology 136**:** 2421-2426.

Pan B, Kong J, Jin J, Kong J, He Y, Dong S, *et al.* (2016). A novel anti-inflammatory mechanism of high density lipoprotein through up-regulating annexin A1 in vascular endothelial cells. BBA - Mol Cell Biol Lipids 1861**:** 501-512.

Paravicini TM, Yogi A, Mazur A, & Touyz RM (2009). Dysregulation of vascular TRPM7 and annexin-1 is associated with endothelial dysfunction in inherited hypomagnesemia. Hypertension 53**:** 423-429.

Perretti M, & D'Acquisto F (2009a). Annexin A1 and glucocorticoids as effectors of the resolution of inflammation. Nature Rev Immunol 9**:** 62-70.

Perretti M, & Dalli J (2009b). Exploiting the annexin A1 pathway for the development of novel anti-inflammatory therapeutics. Br J Pharmacol 158**:** 936-946.

Pourageaud F, & De Mey JGR (1997). Structural properties of rat mesenteric small arteries after 4-wk exposure to elevated or reduced blood flow. Am J Physiol 273**:** H1699-1706.

Prenner SB, & Chirinos JA (2015). Arterial stiffness in diabetes mellitus. Atherosclerosis 238**:** 370-379.

Purvis GSD, Chiazza F, Chen J, Azevedo-Loiola R, Martin L, Kusters DHM, *et al.* (2018). Annexin A1 attenuates microvascular complications through restoration of Akt signalling in a murine model of type 1 diabetes. Diabetologia 61**:** 482-495.

This article is protected by copyright. All rights reserved.

Author Manuscript

Purvis GSD, Collino M, Loiola RA, Baragetti A, Chiazza F, Brovelli M, *et al.* (2019). Identification of AnnexinA1 as an Endogenous Regulator of RhoA, and Its Role in the Pathophysiology and Experimental Therapy of Type-2 Diabetes. Front Immunol 10**:** 571.

Qin CX, Buxton KD, Pepe S, Cao AH, Venardos K, Love JE, *et al.* (2013). Reperfusion-induced myocardial dysfunction is prevented by endogenous annexin-A1 and its N-terminal-derived peptide Ac-ANX-A1(2-26). Br J Pharmacol 168**:** 238-252.

Qin CX, Rosli S, Deo M, Cao N, Walsh J, Tate M, *et al.* (2019). Cardioprotective Actions of the Annexin-A1 N-Terminal Peptide, Ac2-26, Against Myocardial Infarction. Front Pharmacol 10**:** 269.

Qin CX, Yang YH, May L, Gao X, Stewart AG, Tu Y, *et al.* (2015). Cardioprotective potential of annexin-A1 mimetics in myocardial infarction. Pharmacol Ther 148**:** 47-65.

Rackham CL, Vargas AE, Hawkes RG, Amisten S, Persaud SJ, Austin AL, *et al.* (2016). Annexin A1 Is a Key Modulator of Mesenchymal Stromal Cell-Mediated Improvements in Islet Function. Diabetes 65**:** 129-139.

Raskin P, & Mohan A (2010). Emerging treatments for the prevention of type 1 diabetes. Expert Opin Emerg Drugs 15**:** 225-236.

Ritchie RH, Gordon JM, Woodman OL, Cao AH, & Dusting GJ (2005). Annexin-1 peptide Anx-1(2-26) protects adult rat cardiac myocytes from cellular injury induced by simulated ischaemia. Br J Pharmacol 145**:** 495-502.

Ritchie RH, Love JE, Huynh K, Bernardo BC, Henstridge DC, Kiriazis H, *et al.* (2012). Enhanced phosphoinositide 3-kinase(p110α) activity prevents diabetes-induced cardiomyopathy and superoxide generation in a mouse model of diabetes. Diabetologia 55**:** 3369-3381.

Ritchie RH, Sun X, Bilszta JL, Gulluyan LM, & Dusting GJ (2003). Cardioprotective actions of an N-terminal fragment of annexin-1 in rat myocardium in vitro. Eu J Pharmacol 461**:** 171-179.

Santana ABC, de Souza Oliveira TC, Bianconi BL, Barauna VG, Santos EWCO, Alves TP, *et al.* (2014). Effect of high-fat diet upon inflammatory markers and aortic stiffening in mice. Biomed Res Intl 2014**:** 914102.

Sasson AN, & Cherney DZ (2012). Renal hyperfiltration related to diabetes mellitus and obesity in human disease. World J Diabetes 3**:** 1-6.

Schalkwijk CG, Poland DC, van Dijk W, Kok A, Emeis JJ, Dräger AM, *et al.* (1999). Plasma concentration of C-reactive protein is increased in type I diabetic patients without clinical macroangiopathy and correlates with markers of endothelial dysfunction: evidence for chronic inflammation. Diabetologia 42**:** 351-357.

Souza-Smith FM, Katz PS, Trask AT, Stewart JA, Lord KC, Varner KJ, *et al.* (2011). Mesenteric resistance arteries in type 2 diabetic db/db mice undergo outward remodeling. PLoS ONE 6**:** e23337.

This article is protected by copyright. All rights reserved.

Stehouwer CDA, Henry RMA, & Ferreira I (2008). Arterial stiffness in diabetes and the metabolic syndrome: a pathway to cardiovascular disease. Diabetologia 51**:** 527.

Unthank JL, & Bohlen HG (1987). Quantification of intestinal microvascular growth during maturation: techniques and observations. Circ Res 61**:** 616-624.

Wigg SJ, Tare M, Forbes J, Cooper ME, Thomas MC, Coleman HA, *et al.* (2004). Early vitamin E supplementation attenuates diabetes-associated vascular dysfunction and the rise in protein kinase C-β in mesenteric artery and ameliorates wall stiffness in femoral artery of Wistar rats. Diabetologia 47**:** 1038-1046.

Wilkinson IB, Westerbacka J, Yki-Jarvinen H, & Cockcroft JR (2001). Diabetes and arterial stiffness. In Diabetes and Cardiovascular Disease. eds Johnstone M.T., & Veves A. Humana Press: Totowa, NJ, pp 343-360.

Yang YH, Morand EF, Getting SJ, Paul-Clark M, Liu DL, Yona S, *et al.* (2004). Modulation of inflammation and response to dexamethasone by Annexin 1 in antigen-induced arthritis. Arthritis Rheum 50**:** 976-984.

Zieman SJ, Melenovsky V, & Kass DA (2005). Mechanisms, pathophysiology and therapy of arterial stiffness. Arterioscler Thromb Vasc Biol 25**:** 932-942.

Zimmet P, Alberti KG, & Shaw J (2001). Global and societal implications of the diabetes epidemic. Nature 414**:** 782-787.

Author Manuscript

This article is protected by copyright. All rights reserved.

Author Manuscript

Figure Legends

Figure 1. Impact of insulin resistance on body weight, blood glucose and glycated haemoglobin.

A Body weight (g); **B** blood glucose (mM); **C** Endpoint HbA1c (%); **D** plasma insulin (represented as fold compared to *AnxA1*$^{+/+}$ sham group); and glucose tolerance, both **E** over time and **F** area-under-the-curve (AUC) in sham *AnxA1*$^{+/+}$ (black circles, n=10), sham *AnxA1*$^{-/-}$ (black squares, n=7), insulin-resistant (InsRes) *AnxA1*$^{+/+}$ (blue circles, n=6), and insulin-resistant *AnxA1*$^{-/-}$ (blue squares, n=14) male mice. Values are mean ± SEM. **P*<0.05 vs sham *AnxA1*$^{+/+}$, $^{\#}$*P*<0.05 vs *AnxA1*$^{-/-}$ sham mice. *P*<0.05 was considered statistically significant. A, B, E were analysed using repeated-measures two-way ANOVA with Bonferroni *post hoc* analysis. C, D, F were analysed using a two-way ANOVA with Fisher's LSD *post-hoc* analysis.

Figure 2. Impact of insulin resistance on passive mesenteric artery wall parameters.

A Inner and **B** outer diameters, **C** wall thickness and **D** wall CSA over the pressurisation range (5-120mmHg) in sham *AnxA1*$^{+/+}$ (black circles, n=10), sham *AnxA1*$^{-/-}$ (black squares, n=6), insulin-resistant (InsRes) *AnxA1*$^{+/+}$ (blue circles, n=6), and insulin-resistant *AnxA1*$^{-/-}$ (blue squares, n=15) male mice. Values are mean ± SEM. **P*<0.05 vs *AnxA1*$^{+/+}$ sham mice. *P*<0.05 was considered statistically significant. Data were analysed using repeated-measures two-way ANOVA with Bonferroni *post hoc* analysis.

Figure 3. Impact of insulin resistance on passive mechanical wall properties.

This article is protected by copyright. All rights reserved.

A Stress-strain relationships; **B** volume compliance (over the pressurisation range) and **C** AUC for volume compliance; **D** % change in length (over the pressurisation range) in sham *AnxA1*$^{+/+}$ (black circles, n=8), sham *AnxA1*$^{-/-}$ (black squares, n=5), insulin-resistant (InsRes) *AnxA1*$^{+/+}$ (blue circles, n=7), and insulin-resistant *AnxA1*$^{-/-}$ (blue squares, n=14) male mice. Values are mean ± SEM. **P*<0.05 vs sham *AnxA1*$^{+/+}$, §*P*<0.05 vs *AnxA1*$^{+/+}$ insulin-resistant mice. A, B, D were analysed using repeated-measures two-way ANOVA with Bonferroni *post hoc* analysis, whereas C were analysed using two-way ANOVA with Fisher's LSD *post-hoc* analysis. *P*<0.05 was considered statistically significant.

Figure 4. Impact of insulin deficiency on body weight, blood glucose and glycated haemoglobin.

A Body weight (g) and **B** blood glucose (mM) measures during treatment in sham (circles) and insulin-deficient (InsDef; squares) *AnxA1*$^{+/+}$ (black) and *AnxA1*$^{-/-}$ (red) male mice. **C** Endpoint glycated haemoglobin (HbA1c, %) and **D** plasma insulin levels were also determined (represented as fold compared to *AnxA1*$^{+/+}$ sham group). Sham *AnxA1*$^{+/+}$ (black circles, n=10), sham *AnxA1*$^{-/-}$ (black squares, n=7), insulin-deficient *AnxA1*$^{+/+}$ (red circles, n=6), and insulin-deficient *AnxA1*$^{-/-}$ (red squares, n=12) male mice. Values are mean ± SEM. **P*<0.05 vs sham *AnxA1*$^{+/+}$, $^{\#}$*P*<0.05 vs *AnxA1*$^{-/-}$ sham mice. A, B were analysed using repeated-measures two-way ANOVA with Bonferroni *post hoc* analysis. C, D were analysed using a two-way ANOVA with Fisher's LSD *post-hoc* analysis.

Figure 5. Impact of insulin deficiency on passive mesenteric artery wall parameters.

This article is protected by copyright. All rights reserved.

Author Manuscript

A Inner and **B** outer diameters, **C** wall thickness and **D** wall cross-sectional area (CSA) over the pressurisation range (5-120mmHg) in sham *AnxA1*$^{+/+}$ (black circles, n=14), sham *AnxA1*$^{-/-}$ (black squares, n=10), insulin-deficient (InsDef) *AnxA1*$^{+/+}$ (red circles, n=10), and insulin-deficient *AnxA1*$^{-/-}$ (red squares, n=8) male mice. Values are mean ± SEM. $^{\#}P<0.05$ *AnxA1*$^{-/-}$ sham vs. *AnxA1*$^{-/-}$ InsDef; $*P<0.05$ vs sham *AnxA1*$^{+/+}$, $^{\#}P<0.05$ vs *AnxA1*$^{-/-}$ sham mice, $^{\S}P<0.05$ vs *AnxA1*$^{+/+}$ insulin-deficient mice. Data were analysed using repeated-measures two-way ANOVA with Bonferroni *post hoc* analysis.

Figure 6. Impact of insulin deficiency on passive mechanical wall properties.

A Stress-strain relationship; **B** volume compliance (over the pressurisation range) and **C** AUC for volume compliance; **D** % change in length (over the pressurisation range) in sham *AnxA1*$^{+/+}$ (black circles, n=14), sham *AnxA1*$^{-/-}$ (black squares, n=8), insulin-deficient (InsDef) *AnxA1*$^{+/+}$ (red circles, n=13), and insulin-deficient *AnxA1*$^{-/-}$ (red squares, n=8) male mice. Values are mean ± SEM. $^{\#}P<0.05$ vs. all other groups; $*P<0.05$ vs sham *AnxA1*$^{+/+}$, $^{\#}P<0.05$ vs *AnxA1*$^{-/-}$ sham mice, $^{\S}P<0.05$ vs *AnxA1*$^{+/+}$ insulin-deficient mice. A, B, D were analysed using repeated-measures two-way ANOVA with Bonferroni *post hoc* analysis, whereas C were analysed using two-way ANOVA with Fisher's LSD *post-hoc* analysis.

Figure 7. Expression and localisation of the AnxA1/FPR system in insulin-resistant and insulin-deficient mice.

mAnxA1 (A), *mFpr1*, *mFpr2* and *mMCP-1* mRNA expression in mesenteric arteries of insulin-resistant (InsRes, B) and insulin-deficient (InsDef, C) male mice. Sham *AnxA1*$^{+/+}$ and

This article is protected by copyright. All rights reserved.

Author Manuscript

AnxA1$^{-/-}$ (black, n=6); insulin-deficient *AnxA1*$^{+/+}$ and *AnxA1*$^{-/-}$ (red, n=6); insulin-resistant *AnxA1*$^{+/+}$ and *AnxA1*$^{-/-}$ (blue, n=6) male mice. Localisation (representative image) and quantification of FPRs in mesenteric arteries (D, n=5-7). Insert highlights a region within the blood vessel (magnification X100). VSMCs, vascular smooth muscle cells; EC, endothelial cell; *mFpr1*, formyl peptide receptor 1 gene; *mFpr2*, formyl peptide receptor 2 gene; FPR1, formyl peptide receptor 1 protein; FPR2, formyl peptide receptor 2 protein. Values are mean ± SEM. An outlier in insulin-deficient *AnxA1*$^{-/-}$ mice is predefined when an individual data point is 2 standard deviations away from the mean. **P*<0.05. A was analysed using unpaired Student's t-test, B, C were analysed using repeated-measures two-way ANOVA with Bonferroni *post hoc* analysis, D was analysed using a Mann-Whitney test.

Figure 8. Summary of the role of endogenous Annexin-A1 in the context of insulin resistance versus insulin deficiency.

AnxA1 deficiency decreases vessel compliance in insulin-resistant mice. Conversely, AnxA1 deficiency has no impact on vessel compliance in normal and insulin-deficient mice. Schema created using a modification to an image provided by Servier Medical Art by Servier (http://www.servier.com/Powerpoint-image-bank), licenced using a Creative Commons Attributes 3.0 Unported Licence (http://creativecommons.com/licence/by/3.0).

This article is protected by copyright. All rights reserved.

Author Manuscript

Author Manuscript

Table 1. Blood pressure and heart rate in insulin-resistant and insulin-deficient *AnxA1*$^{+/+}$ and *AnxA1*$^{-/-}$ male mice. SBP, systolic blood pressure; DBP, diastolic blood pressure; HR, heart rate. Values are mean ± SEM with *n* indicated in brackets. *****$P < 0.05$ indicates reduced vs. sham *AnxA1*$^{+/+}$, $^{\#}P < 0.05$ indicates increased vs. sham *AnxA1*$^{+/+}$. Data were analysed using two-way ANOVA with Fisher's LSD *post-hoc* analysis.

	Insulin-resistant study				**Insulin-deficient study**			
	Sham		**Insulin resistant**		**Sham**		**Insulin-deficient**	
	AnxA1$^{+/+}$	*AnxA1*$^{-/-}$	*AnxA1*$^{+/+}$	*AnxA1*$^{-/-}$	*AnxA1*$^{+/+}$	*AnxA1*$^{-/-}$	*AnxA1*$^{+/+}$	*AnxA1*$^{-/-}$
SBP (mmHg)	97±2 (10)	107±6 (6)	107±6 (5)	123±5 (13)	117±6 (8)	116±5 (7)	93±3***** (5)	95±5***** (5)
DBP (mmHg)	66±2 (10)	70±4 (6)	68±7 (5)	81±3 (13)	74±4 (8)	79±4 (7)	63±2 (5)	63±7 (5)
HR (BPM)	409±4 (10)	401±10 (6)	404±13 (5)	446±14$^{\#}$ (13)	401±8 (8)	404±13 (7)	399±20 (5)	412±19 (5)

This article is protected by copyright. All rights reserved.

Author Manuscript

Table 2. Summary of the phenotypes of insulin-resistant and insulin-deficient *AnxA1*$^{+/+}$ and *AnxA1*$^{-/-}$ male mice compared with *AnxA1*$^{+/+}$ sham controls. GTT, glucose tolerance test; HbA1c, glycated haemoglobin; ND, not determined.

	Insulin-resistant study			**Insulin-deficient study**		
	***AnxA1*$^{-/-}$ sham**	***AnxA1*$^{+/+}$ InsRes**	***AnxA1*$^{-/-}$ InsRes**	***AnxA1*$^{-/-}$ sham**	***AnxA1*$^{+/+}$ InsDef**	***AnxA1*$^{-/-}$ InsDef**
Body weight	↔	↔	↔	↔	↓	↓↓
Blood glucose	↔	↑	↑	↔	↑↑	↑↑
GTT	↔	↑	↑	ND	ND	ND
HbA1c	↔	↑	↔	↔	↑	↑
Plasma insulin	↔	↔	↔	↓	↓	↓
Systolic blood pressure	↔	↔	↔	↔	↓	↓
Heart rate	↔	↔	↑	↔	↔	↔
Vascular Remodelling	None	Outward (hypertrophic)	None	None	Outward (hypertrophic)	Outward (eutrophic)
Circumferential stiffness	↔	↔	↔	↔	↔	↓
Volume compliance	↓	↔	↓	↔	↑	↑
Arterial lengthening	↓	↓	↓	↔	↑	↔

This article is protected by copyright. All rights reserved.

Author Manuscript

This article is protected by copyright. All rights reserved.

Author Manuscript

Figure 1

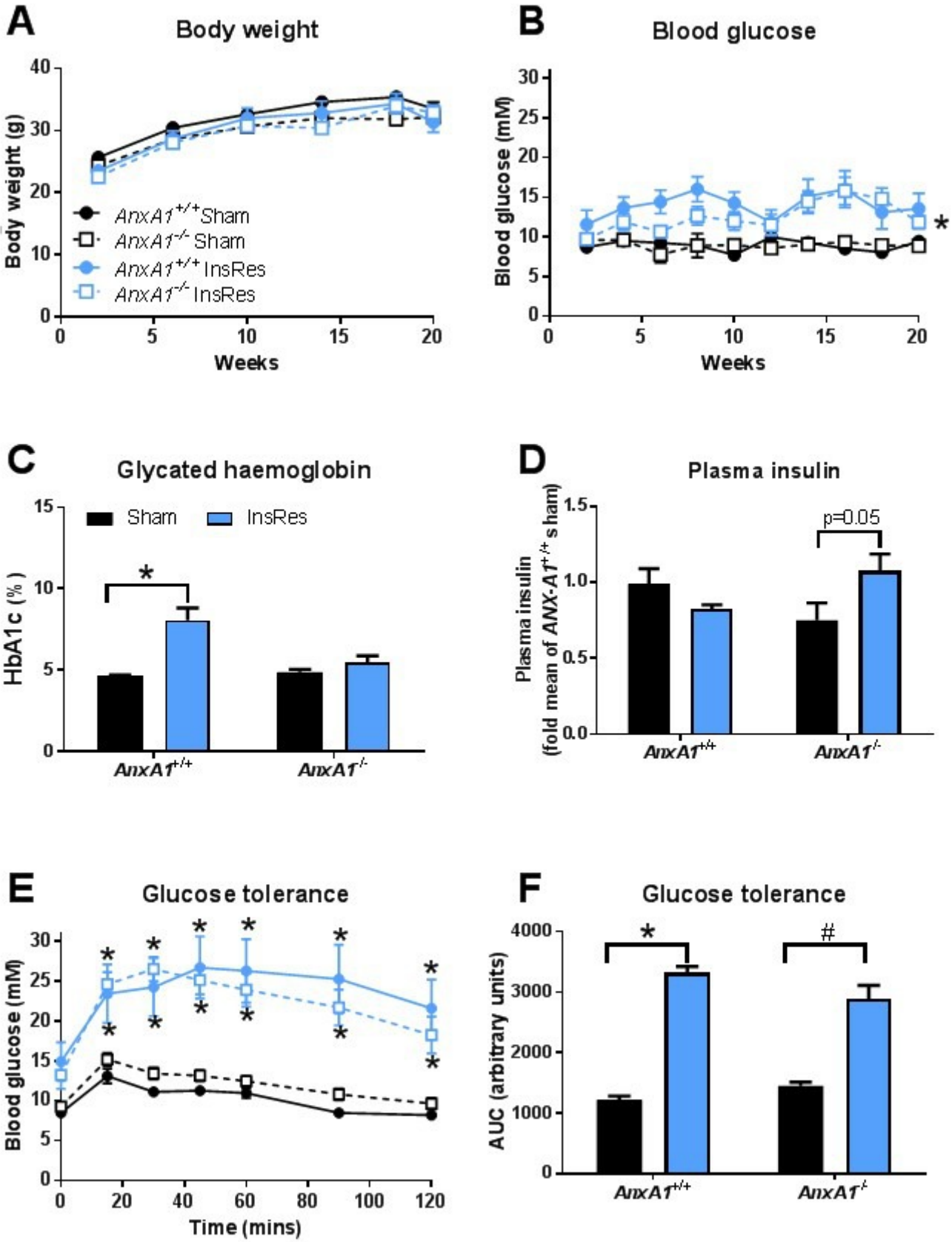

BPH_14927_fig 1.JPG

This article is protected by copyright. All rights reserved.

Figure 2

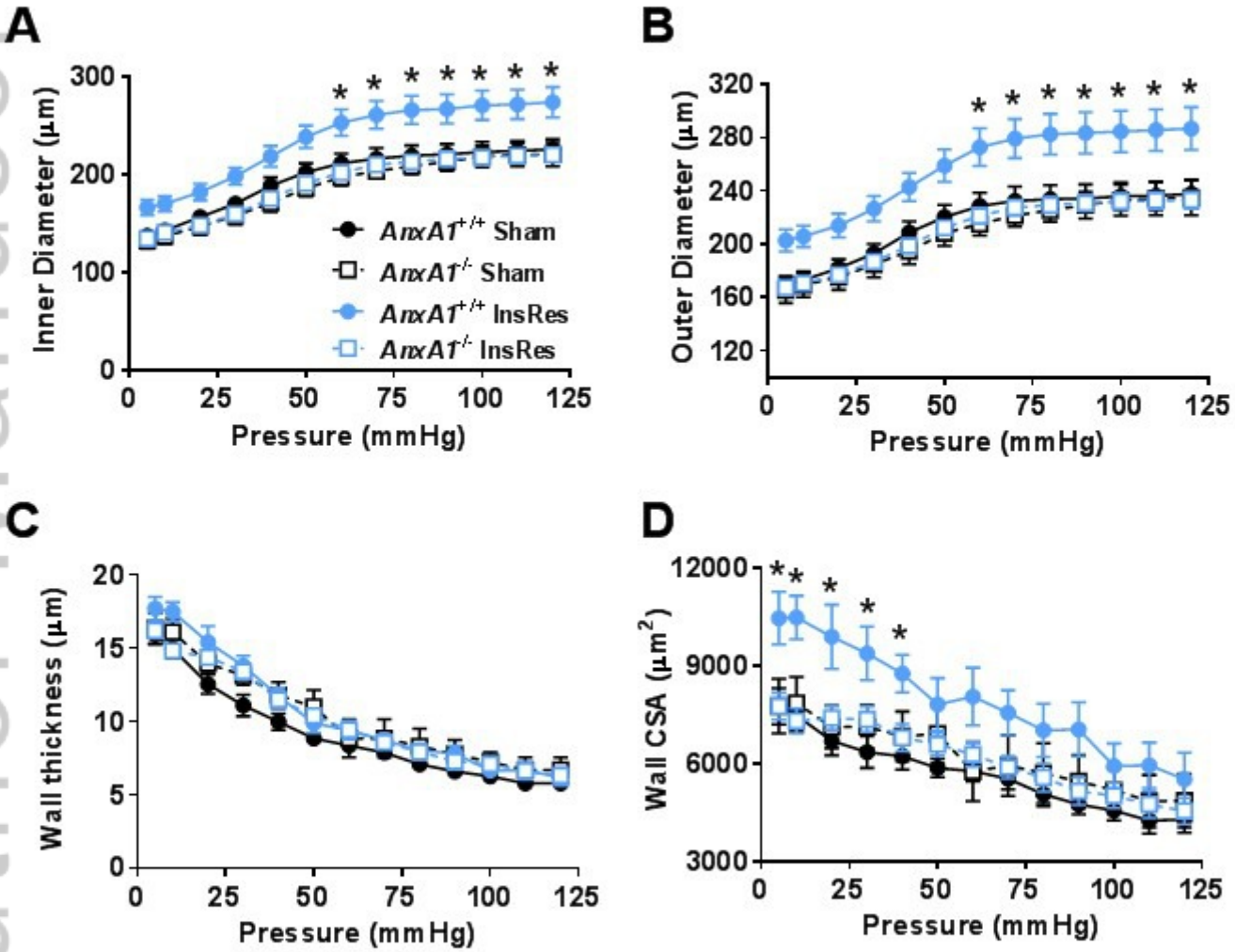

BPH_14927_Fig 2.JPG

This article is protected by copyright. All rights reserved.

Author Manuscript

Figure 3

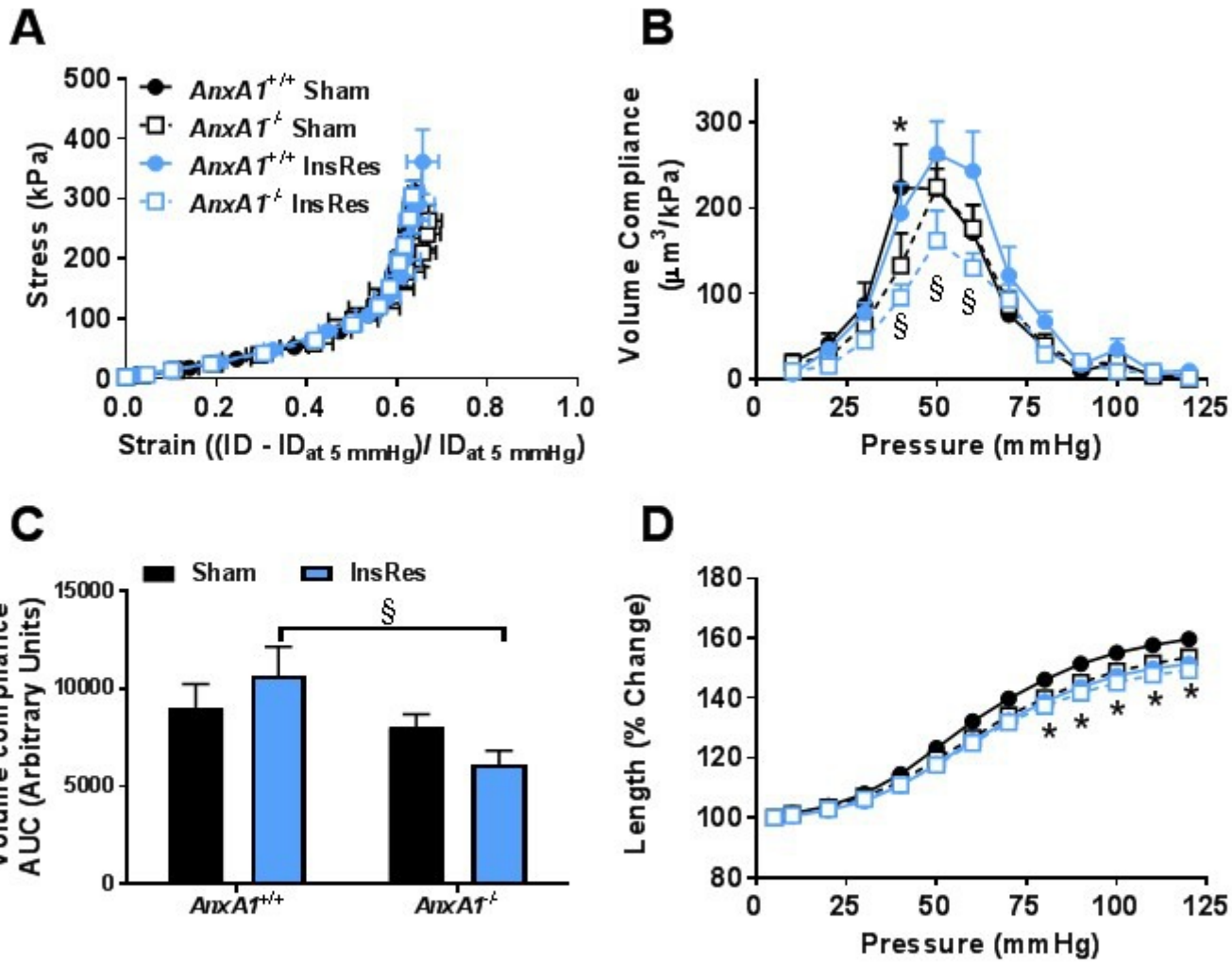

Author Manuscript

This article is protected by copyright. All rights reserved.

Figure 4

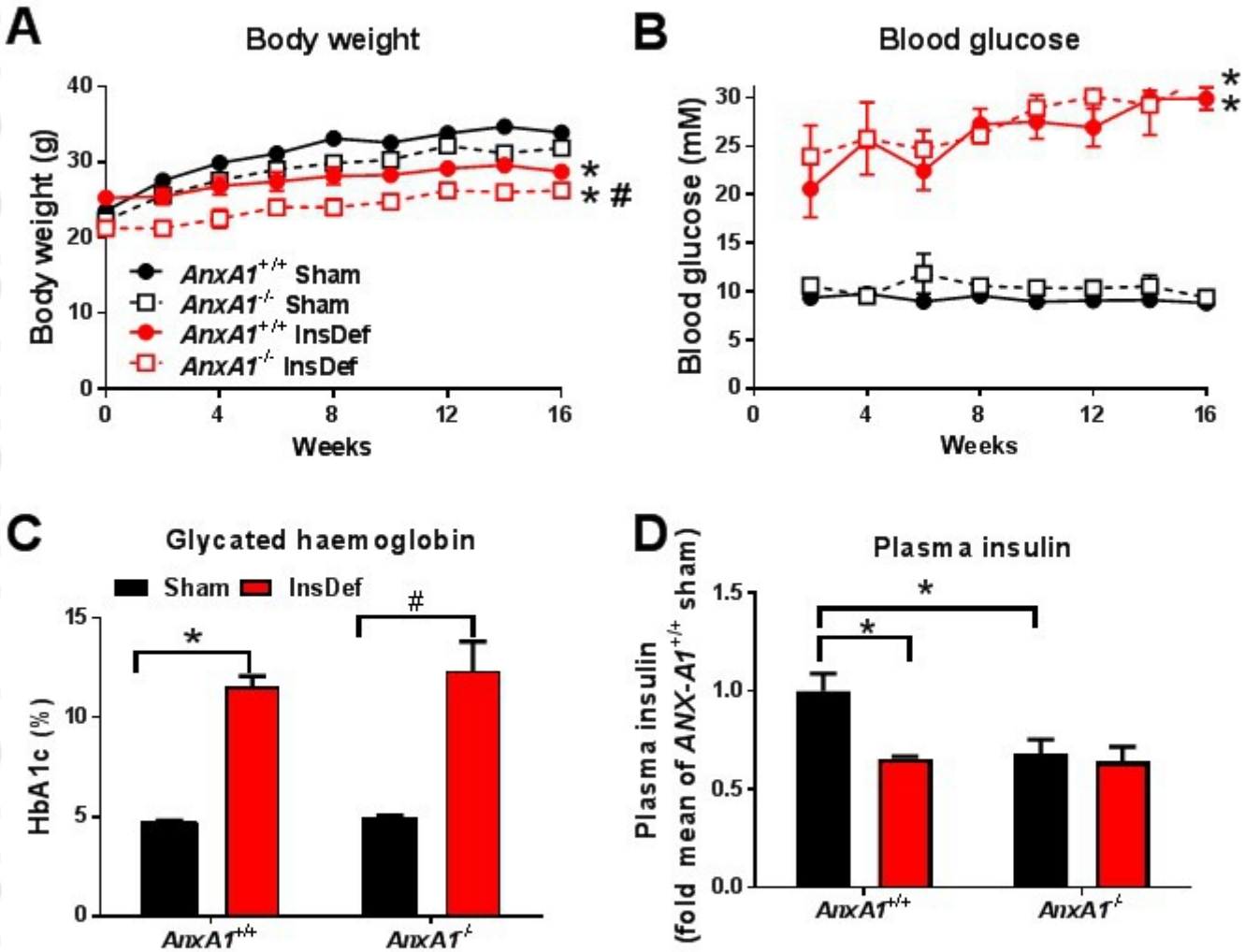

Author Manuscript

This article is protected by copyright. All rights reserved.

Figure 5

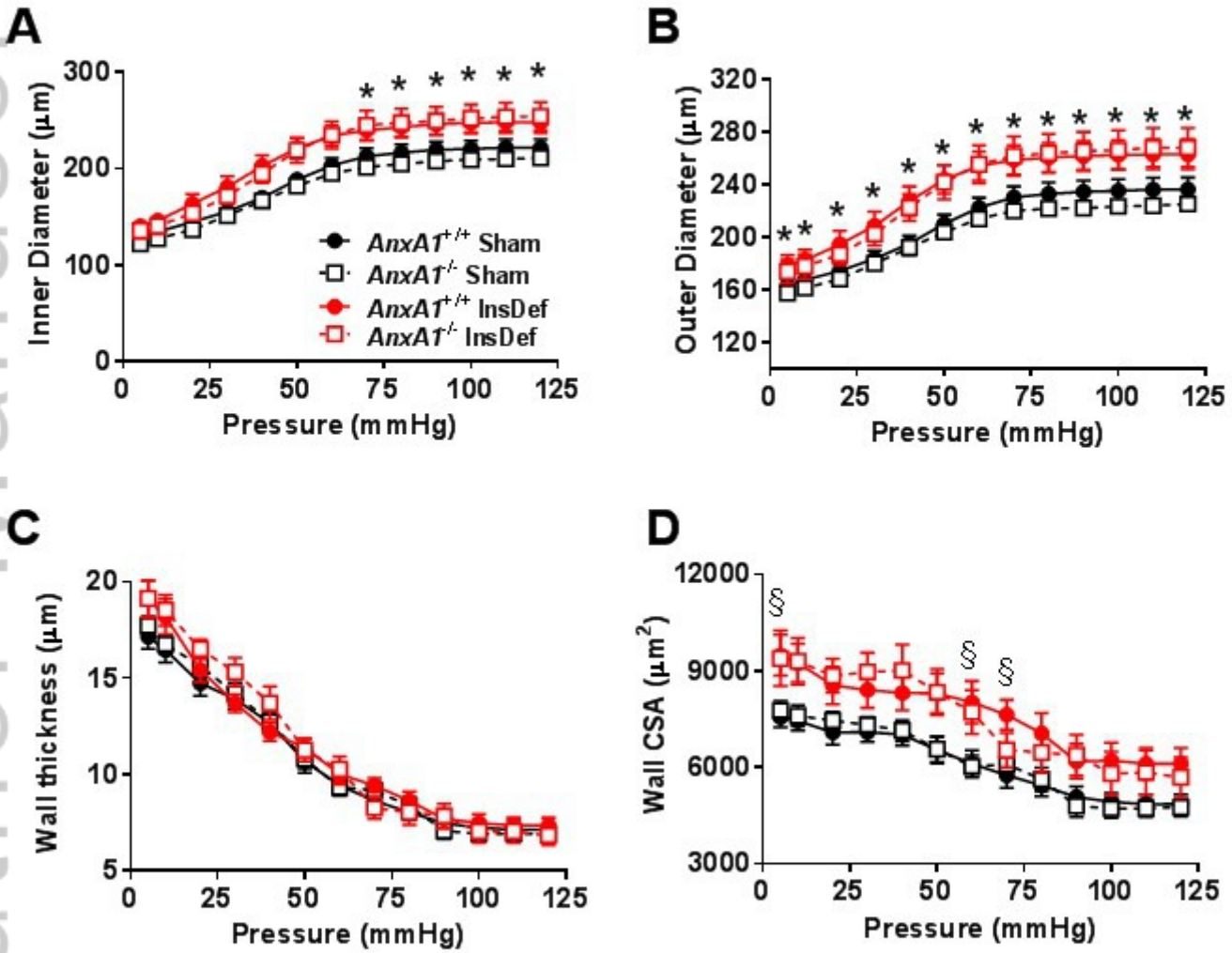

Author Manuscript

This article is protected by copyright. All rights reserved.

Author Manuscript

Figure 6

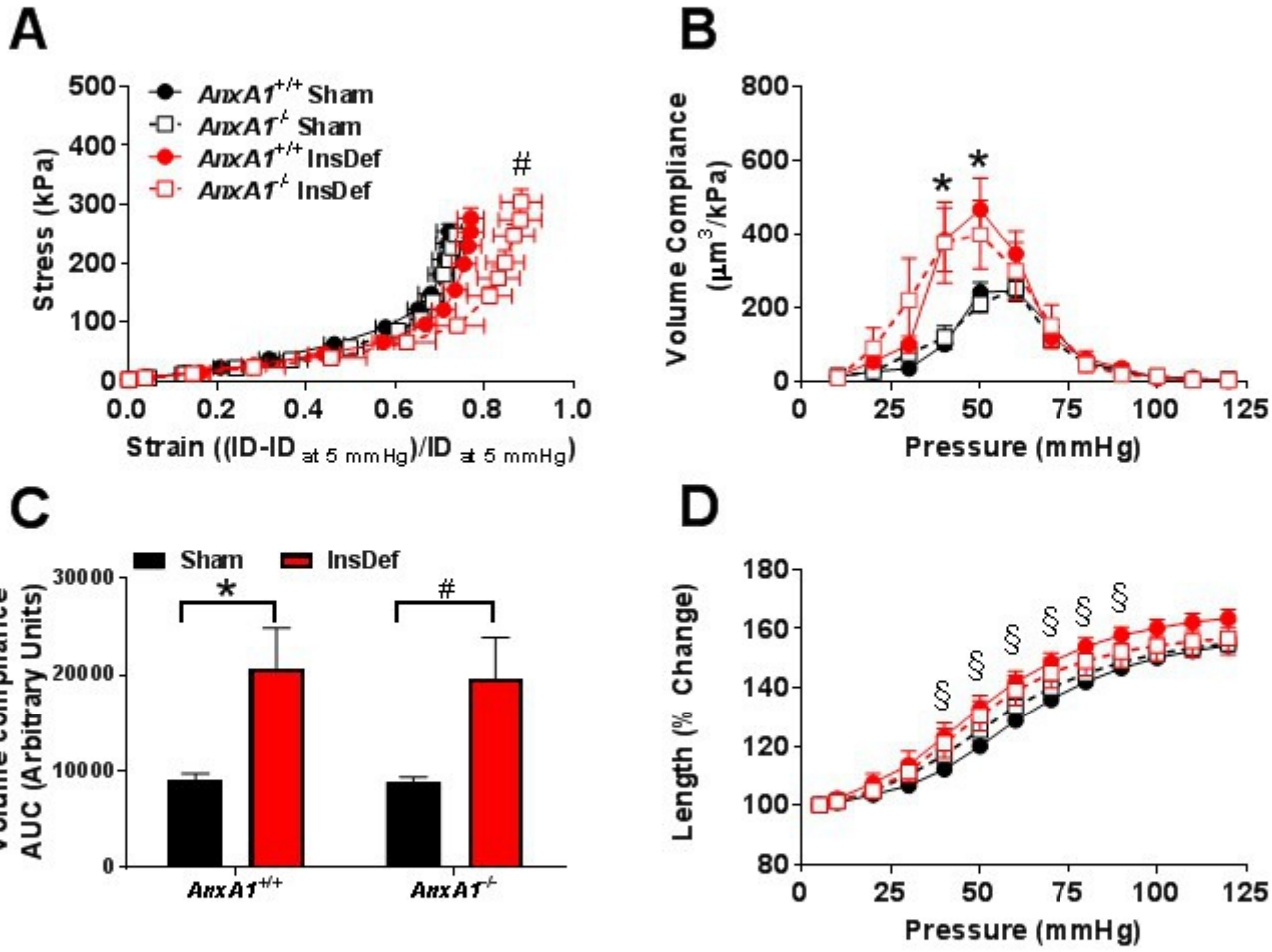

BPH_14927_Fig 6.JPG

This article is protected by copyright. All rights reserved.

Figure 7

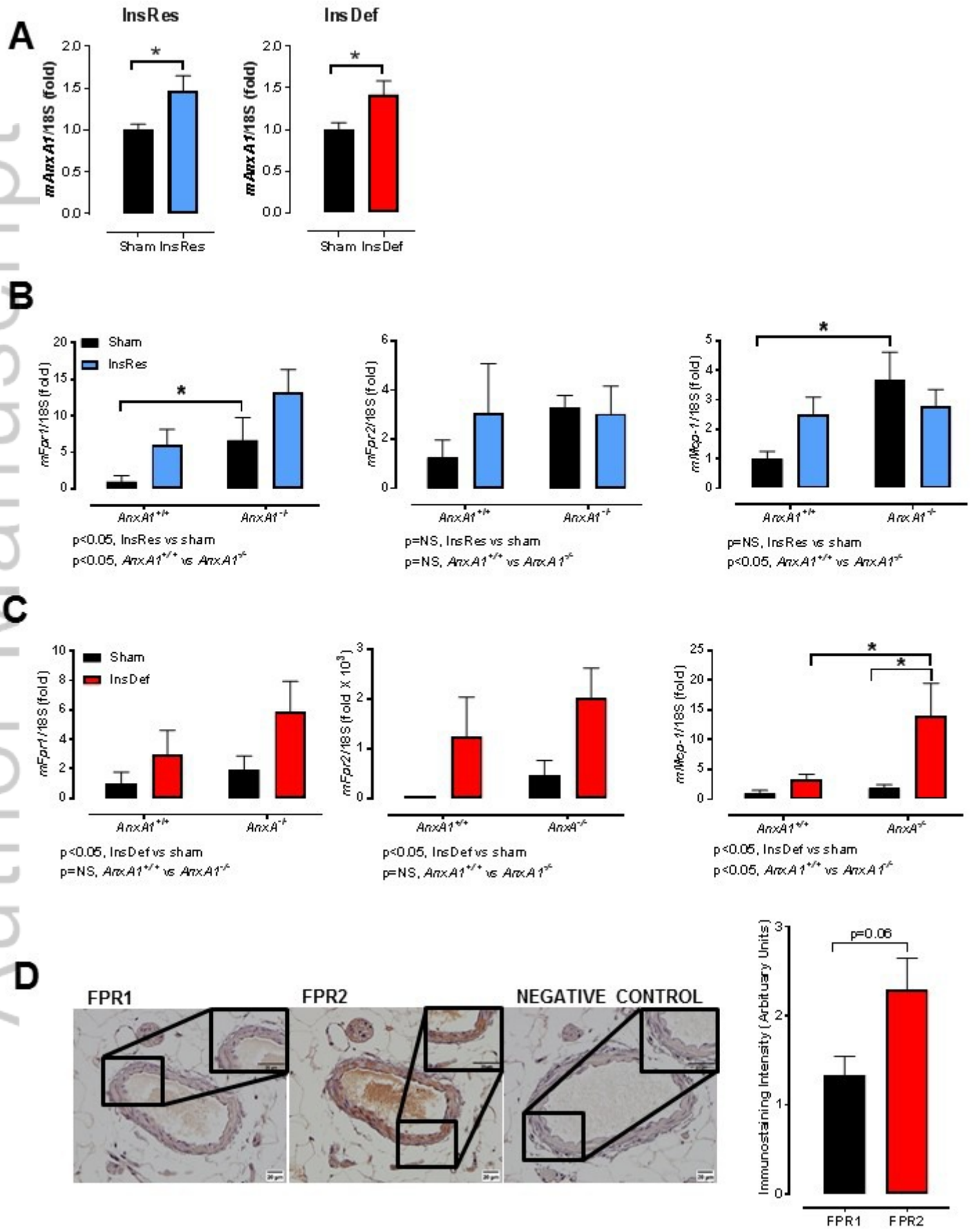

BPH_14927_Fig 7.JPG

This article is protected by copyright. All rights reserved.

Author Manuscript

Figure 8

A. Schematic summary of the impact of Anx-A1 deficiency on insulin-resistant and insulin-deficient vasculature.

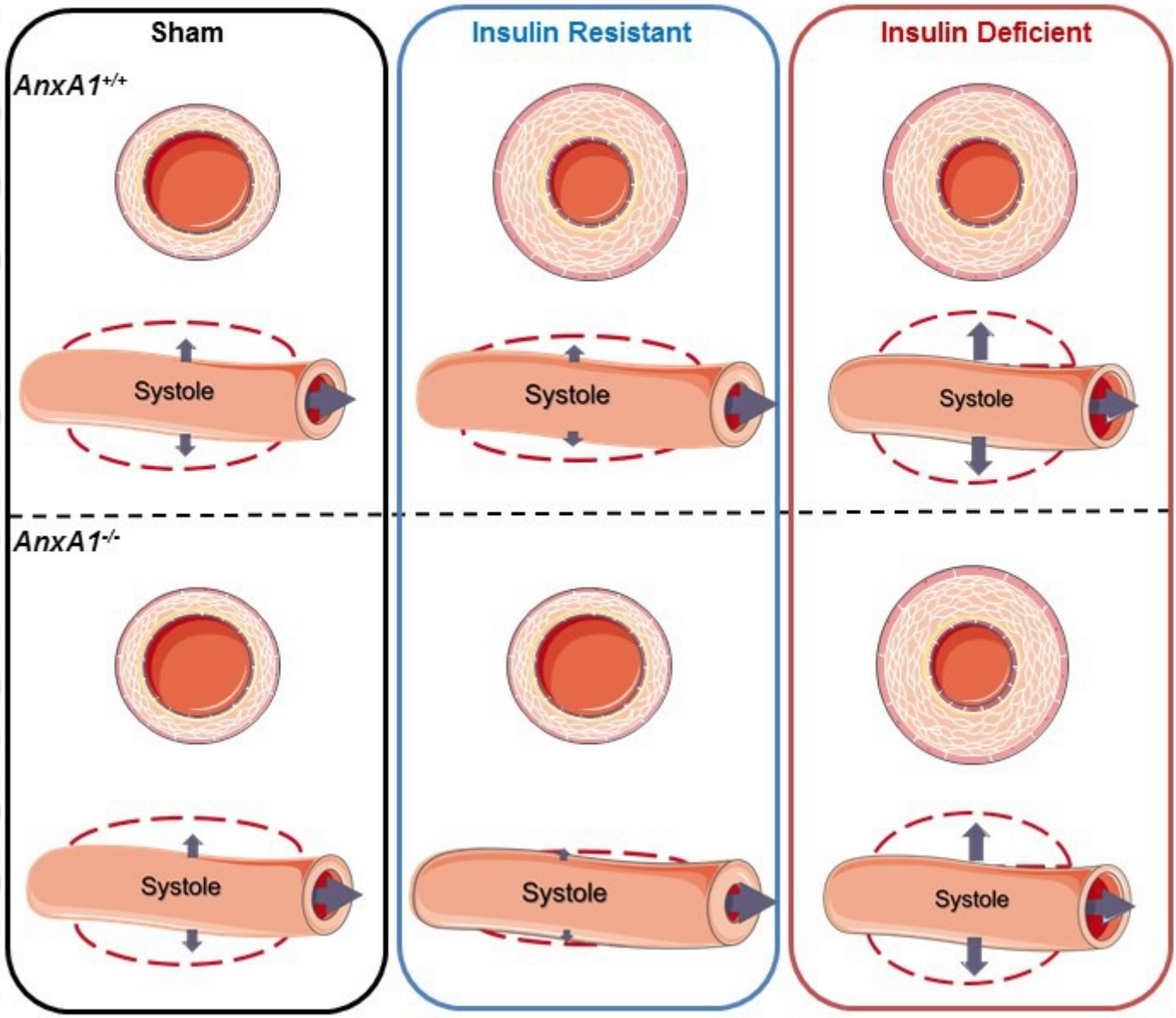

Author Manuscript

BPH_14927_Fig 8.JPG

This article is protected by copyright. All rights reserved.